Protein J (2011) 30:220–227
DOI 10.1007/s10930-011-9323-3

Stereoselective Inhibition of Cholesterol Esterase by Enantiomers of *exo*- and *endo*-2-Norbornyl-*N*–*n*-butylcarbamates

Ming-Cheng Lin · Shyh-Jei Yeh · I-Ru Chen · Gialih Lin

Published online: 31 March 2011

Abstract Four stereoisomers of 2-norbornyl-*N*–*n*-butylcarbamates are characterized as the pseudo substrate inhibitors of cholesterol esterase. Cholesterol esterase shows enantioselective inhibition for enantiomers of *exo*- and *endo*-2-norbornyl-*N*–*n*-butylcarbamates. For the inhibitions by (*R*)-(+)- and (*S*)-(−)-*exo*-2-norbornyl-*N*–*n*-butylcarbamates, the *R*-enantiomer is 6.8 times more potent than the *S*-enantiomer. For the inhibitions by (*R*)-(+)- and (*S*)-(−)-*endo*-2-norbornyl-*N*–*n*-butyl-carbamates, the *S*-enantiomer is 4.6 times more potent than the *R*-enantiomer. The enzyme-inhibitor complex models have been proposed to explain these different enantioselectivities.

Keywords Cholesterol esterase · Inhibitors · Carbamates · Enantiomers

Abbreviations

ACS	Acyl chain binding site
CEase	Cholesterol esterase
LDL	Low-density lipoprotein
PNPB	*p*-nitrophenyl butyrate
TX	Triton-X 100

M.-C. Lin
Department of Internal Medicine, Chung Shan Medical University Hospital, School of Medicine, Chung-Shan Medical University, Taichung 402, Taiwan

S.-J. Yeh · I.-R. Chen · G. Lin (✉)
Department of Chemistry, National Chung-Hsing University, Taichung 402, Taiwan
e-mail: gilin@dragon.nchu.edu.tw

1 Introduction

Cholesterol esterase (CEase, EC 3.1.1.13) also known as bile salt-activated lipase, carboxyl ester lipase, lysophospholipase, and non-specific lipase, is responsible for the hydrolysis of dietary cholesterol esters, fat soluble vitamin esters, phospholipids and triacylglycerols. Like the serine proteases, CEase possesses a catalytic triad, Ser194-His435-Asp320, that serves as a nucleophilic and general acid–base catalytic entity [12, 14, 22]. Two X-ray structures of CEase have been reported [4, 23]. Although different bile salt-activation mechanisms are proposed, the active site of CEase from two different X-ray crystal structures is similar to that of lipases.

CEase has also been demonstrated that it is involved directly in lipoprotein metabolism, in that the enzyme catalyzes the conversion of large low-density lipoprotein (LDL) to smaller, denser, more cholesterol ester-rich lipoproteins, and that the enzyme may regulate serum cholesterol levels [3]. Therefore, the ability of CEase to convert large LDL to smaller LDL subspecies, and the relationship between plasma CEase and LDL levels, suggest that high plasma CEase levels may constitute a potential risk factor for atherosclerosis. Thus, CEase inhibitors may be suitable for the treatment of combined lipoprotein disorders characterized by elevation of cholesterol [1, 7, 15, 19].

Carbamate inhibitors have been characterized as the pseudo substrate inhibitors of CEase (Scheme 1) [9–11]. We have synthesized (*R*)-(+)-*exo*-, (*S*)-(−)-*exo*-, (*R*)-(+)-*endo*-, and (*S*)-(−)-*endo*-2-norbornyl-*N*–*n*-butylcarbamates (Fig. 1) from optically pure (*R*)-(+)-*exo*-, (*S*)-(−)-*exo*-, (*R*)-(+)-*endo*-, and (*S*)-(−)-*endo*-2-norborneols which are kinetically resolved by porcine pancreatic lipase in organic solvent (Schemes 2, 3, 4) [5, 6]. (*R*)-(+)-*exo*-,

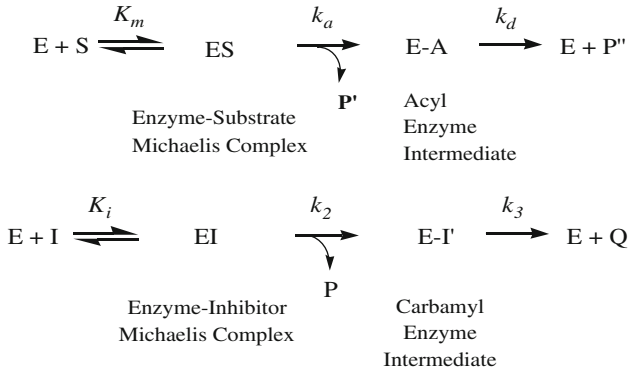

Scheme 1 Kinetic scheme for pseudo substrate inhibitions of CEase by carbamate inhibitors in the presence of substrate. E: enzyme, CEase; E-A: acyl enzyme; EI: enzyme-inhibitor Michaelis complex; E-I′: carbamyl enzyme; ES: enzyme-substrate Michaelis complex; I: pseudo substrate inhibitor; k_2: carbamyl constant; k_3: decarbamylation constant; k_a: acylation constant; k_{cat}: turnover number = $k_a k_d/(k_a + k_d)$; k_d: deacylation constant; K_i: inhibition constant; K_m: Michaelis–Menten constant; P: product, 2-norborneol; P′: product, *p*-nitrophenol; P″: product, butyrate; Q: product, butylcarbamic acid; S: substrate, PNPB

(*S*)-(−)-*exo*-, (*R*)-(+)-*endo*-, and (*S*)-(−)-*endo*-2-Norbornyl *N*–*n*-butylcarbamates have shown high enantioselectivity for the inhibition of acetylcholinesterase and butyrylcholinesterase. In this paper, we further study the stereoselectivity for cholesterol esterase inhibition by these chiral norbornyl-derived carbamates.

2 Materials and Methods

2.1 Materials

Porcine pancreatic lipase (PPL), porcine pancreatic CEase, *p*-nitrophenyl butyrate (PNPB), and triton-X 100 (TX) were obtained from Sigma. (±)-*exo*- and (±)-*endo*-2-Norborneol, *n*-butyl isocyanate, triethylamine, $CDCl_3$, tetramethylsilane, *t*-butyl methyl ether, butanol, vinyl acetate, butyryl chloride, pyridine, and (*S*)-(+)-α-methoxy-α-trifluoromethylphenylacetyl chloride were purchased from Aldrich (USA). Silica gel and TLC plate were obtained from Merck (Germany). Hexane, CH_2Cl_2, ethyl acetate, and tetrahydrofuran were obtained from TEDIA (USA). Sodium dihydrogen phosphate ($NaH_2PO_4{:}2H_2O$), disodium hydrogen phosphate ($Na_2HPO_4{:}12H_2O$), hydrogen chloride (HCl), sodium hydroxide (NaOH), potassium hydroxide (KOH), calcium chloride ($CaCl_2$), and sodium chloride (NaCl) were purchased from UCW (Taiwan). Ethanol (95%) was obtained from Taiwan Tobacco & Liquid Corporation (Taiwan). All other chemicals were of the highest purity available commercially.

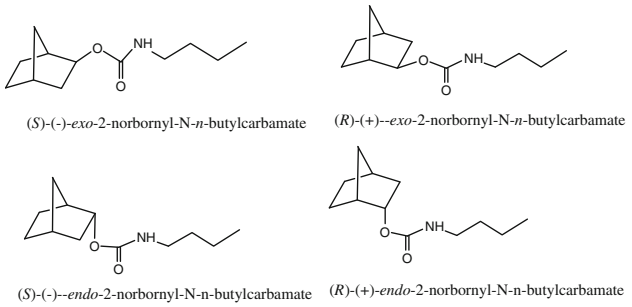

Fig. 1 Structures of (*R*)-(+)-*exo*-, (*S*)-(−)-*exo*-, (*R*)-(+)-*endo*-, (*S*)-(−)-*endo*-2-norbornyl-*N*–*n*-butylcarbamates

2.2 Synthesis of Inhibitors

2.2.1 Kinetic resolution of (S)-(−)-exo- and (R)-(+)-exo-2-norborneol (Scheme 2) [5, 6])

To a *t*-butyl methyl ether (100 mL) solution of racemic (±)-*exo*-2-norbornyl butyrate (1.82 g, 10 mmol) (synthesis from condensation of (±)-*exo*-2-norborneol with 1.2 eqs. of butyryl chloride in the presence of pyridine in CH_2Cl_2, 90–95% yield), porcine pancreatic lipase (4 g) was added. The reaction mixture was shaken at 36 °C at 200 rpm for 72 h. The reaction mixture was evaporated to dryness and was poured into a silica gel column. The product (*S*)-(−)-*exo*-2-norborneol (549 mg, 4.9 mmol) and recovered unreactive (*R*)-*exo*-2-norbornyl butyrate (930 mg, 5.1 mmol) were separated by liquid chromatography eluted by hexane–ethyl acetate solvent gradient. This reaction yielded (*S*)-(−)-*exo*-2-norborneol (49% yield) (mp = 125–126 °C and $[\alpha]_D^{25} = -2.70^o$; $[\alpha]_D^{25} = -3.07^o$ and mp = 126–127 °C from literature) [2, 13, 16, 24, 25] and recovered unreactive (*R*)-*exo*-2-norbornyl butyrate (51% yield). (*R*)-(+)-*exo*-2-Norborneol (mp = 125–126 °C and $[\alpha]_D^{25} = +2.70^o$) ($[\alpha]_D^{25} = +3.06^o$ and mp = 126–127 °C from literature) was obtained from basic hydrolysis (0.1 M KOH) of (*R*)-*exo*-norbornyl butyrate in ethanol (95% v/v) in 99% yield. To a 0.1 M KOH ethanol (95% v/v) solution (50 mL), (*R*)-*exo*-2-norbornyl butyrate (500 mg, 2.75 mmol), was added and stirred at 25 °C for 18 h. The reaction mixture was evaporated to dryness and was poured into a silica gel column. The product (*R*)-(+)-*exo*-2-norborneol (300 mg, 2.7 mmol) was isolated from liquid chromatography by hexane–ethyl acetate solvent gradient in 99% yield.

The enantiomeric excess (e.e.) values of (*R*)-(+)-*exo*- and (*S*)-(−)-*exo*-2-norborneols from the resolutions were calculated to be 80 and 84%, respectively, from the ^{19}F NMR spectra of their Mosher's esters as the followings (Table 1) [8, 20, 21]. In an NMR tube containing 1 mL of $CDCl_3$, (*R*)-(+)-*exo*-2-norborneol (5.6 mg, 50 μmol) was condensed with the Mosher's chiral derivatizing agent (*S*)-(+)-α-methoxy-α-trifluoromethyl-phenylacetyl chloride

Scheme 2 Kinetic resolution of (*R*)-(+)- and (*S*)-(−)-*exo*-2-norborneols from lipase catalyzed hydrolysis of racemic (±)-*exo*-2-norbornyl butyrate

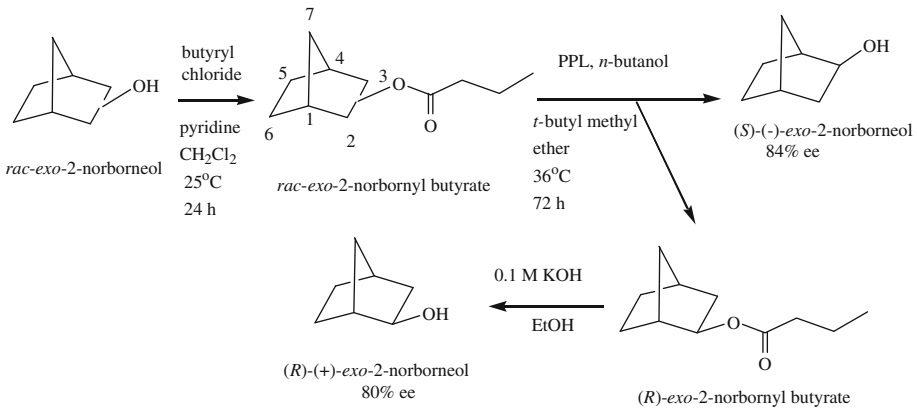

Scheme 3 Kinetic resolution of (*R*)-(+)- and (*S*)-(−)-*endo*-2-norborneols from lipase catalyzed acetylation of racemic (±)-*exo*-2-norborneol with vinyl acetate

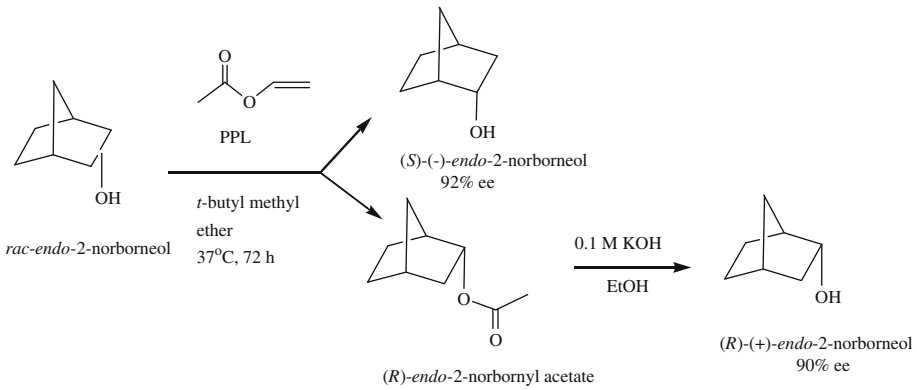

Scheme 4 Determination of enantiomeric excess and absolute configuration of (*R*)-(+)- and (*S*)-(−)-*exo*-2-norborneols by ^{19}F NMR spectra of their Mosher's ester derivatives

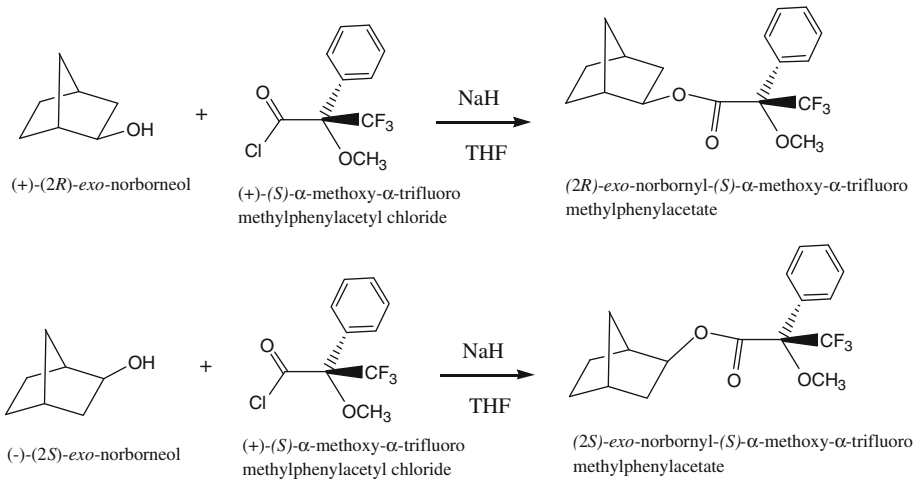

[8] (12.6 mg, 50 μmol) in $CDCl_3$ in the presence of pyridine (10 μL) at 25 °C for 24 h (Scheme 4). The fluorine chemical shifts at −73.948 and −74.113 ppm with the integration ratio of 9/1 were assigned to be the fluorine atoms of *(R)- and (S)-exo*-2-norbornyl-(*S*)-α-methoxy-α-trifluoromethylphenyl acetates, respectively. The enantiomeric excess of (*R*)-(+)-*exo*-2-norborneol from the kinetic resolution by lipase catalysis was calculated to be 80% from integration of these two ^{19}F NMR peaks (Table 1).

The enantiomeric excess of (*S*)-(+)-*exo*-2-norborneol from the kinetic resolution by lipase catalysis was calculated to be 84% in a similar method described for (*R*)-(−)-*exo*-2-norborneol (Table 1).

2.2.2 *Kinetic resolution of (S)-(−)-endo- and (R)-(+)-endo-2-norborneol (Scheme 3) [5, 6]*

To a *t*-butyl methyl ether (50 mL) solution of racemic (±)-*endo*-2-norborneol (5 g, 44.6 mmol) and vinyl acetate

Table 1 Enantiomeric excess (%) and optical purity (%) for the kinetic resolution of racemic *exo*-2-norborneol and *endo*-2-norborneol by lipase in organic solvent

Compound	Enantiomeric excess (%)[a]	Optical purity (%)[b]
(*R*)-(+)-*exo*-2-norborneol	80	88
(*S*)-(−)-*exo*–2-norborneol	84	90
(*R*)-(+)-*endo*-2-norborneol	90	96
(*S*)-(−)-*endo*-2-norborneol	92	96

[a] Enantiomeric excess (%) was calculated from ratio of integration of fluorine chemical shift of their Mosher's ester derivatives of ^{19}F NMR spectra (Scheme 4)

[b] Optical purity (%) was calculated as 100 × $[\alpha]^{25}_{D\,observed}/[\alpha]^{25}_{D\,literature}$

(9.34 g, 108.6 mmol), porcine pancreatic lipase (30 g) was added. The reaction mixture was shaken at 37 °C at 200 rpm for 72 h. The reaction mixture was evaporated to dryness and was poured into a silica gel column. The product (*R*)-(+)-*endo*-2-norbornyl acetate (3.36 g, 21.8 mmol) and recovered unreactive (S)-(−)-*endo*-norborneol (2.55 g, 22.7 mmol) were separated by liquid chromatography eluted by hexane–ethyl acetate solvent gradient. This reaction yielded (*R*)-(+)-*endo*-2-norbornyl acetate (49%) and recovered unreactive (S)-(−)-*endo*- norborneol (51%) (mp = 148–150 °C and $[\alpha]^{25}_{D} = -1.81^{o}$; mp = 151–152 °C and $[\alpha]^{25}_{D} = -1.89^{o}$ from literature) [2, 13, 16, 24, 25]. (*R*)-(+)-*endo*-2-Norborneol (mp = 148–150 °C and $[\alpha]^{25}_{D} = +1.81$; $[\alpha]^{25}_{D} = +1.89^{o}$ and mp = 151–152 °C from literature) was obtained from basic hydrolysis (0.1 M KOH) of (*R*)-*endo*-norbornyl acetate in ethanol (95%) in 99% yield. To a 0.1 M KOH ethanol (95% v/v) solution (50 mL), (*R*)-(+)-*endo*-2-norbornyl acetate (3 g, 19.4 mmol), was added and stirred at 25 °C for 18 h. The reaction mixture was evaporated to dryness and was poured into a silica gel column. The product (*R*)-(+)- *endo*-2-norborneol (2.16 g, 19.3 mmol) was isolated from liquid chromatography by hexane–ethyl acetate solvent gradient in 99% yield. The enantiomeric excess (e.e.) values of (*S*)-(−)-*endo*- and (*R*)-(+)-*endo*-2-norborneols from the resolutions were calculated to be 90 and 92%, respectively, from the ^{19}F NMR spectra of their Mosher's esters (Table 1).

In an NMR tube containing 1 mL of $CDCl_3$, (*R*)-(+)-*endo*-2-norborneol (5.6 mg, 50 μmol) was condensed with the Mosher's chiral derivatizing agent (*S*)-(+)-α-methoxy-α-trifluoromethylphenylacetyl chloride (12.6 mg, 50 μmol) in $CDCl_3$ in the presence of pyridine (10 μL) at 25 °C for 24 h. The fluorine chemical shifts at -73.975 and -74.152 ppm with the integration ratio of 95/5 were assigned to be the fluorine atoms of *(2R)*- and *(2S)-endo*-norbornyl-(*S*)-α-methoxy-α-trifluoromethylphenyl acetates, respectively. Therefore, the enantiomeric excess of (*R*)-(+)-*endo*-2-norborneol from the kinetic resolution by lipase catalysis was calculated to be 90% from integration of these two peaks (Table 1).

The enantiomeric excess of (*S*)-(−)-*endo*-2-norborneol from the kinetic resolution by lipase catalysis was calculated to be 92% in a similar method described for (*R*)-(+)-*endo*-2-norborneol (Table 1).

2.2.3 *Synthesis of (R)-(+)-exo-, (S)-(−)-exo-, (R)-(+)-endo-, and (S)-(−)-endo- 2-norbornyl-N–n-butylcarbamates*

(*R*)-(+)-*exo*-, (*S*)-(−)-*exo*-, (*R*)-(+)-*endo*-, and (*S*)-(−)-*endo*-2-norbornyl-*N*–*n*-butylcarbamates (800 mg, 3.8 mmol) were synthesized from condensation of optically pure (*R*)-(+)-*exo*-, (*S*)-(−)-*exo*-, (*R*)-(+)-*endo*-, and (*S*)-(−)-*endo*-2-norborneols (500 mg, 4.46 mmol), respectively, with 1.2 eqs. of *n*-butyl isocyanate (5.36 mmol) in the presence of 1.2 eqs. of triethylamine (5.36 mmol) in tetrahydrofuran (50 mL) at 25° C for 1 day (85–92% yield). All products were purified by liquid chromatography (silica gel, hexane–ethyl acetate) and were characterized by ^{1}H and ^{13}C NMR spectra, mass spectra, and elemental analysis as the followings.

(*R*)-(+)-*exo*- and (*S*)-(−)-*exo*-2-norbornyl-*N*–*n*-butycarbamates. ^{1}H NMR ($CDCl_3$) δ 0.92 (t, J = 7 Hz, 3H, carbamate ω-CH_3), 1.40 (sextet, J = 7 Hz, 2H, carbamate γ-CH_2), 1.0–1.6 (m, 7H, 4,5,6,7-norbornyl *H*s), 1.56 (quintet, J = 7 Hz, 2H, carbamate β-CH_2), 1.70 (m, 1H, norbornyl C(1)*H*), 2.24 (m, 2H, norbornyl C(3)H_2), 3.15 (t, J = 7 Hz, 2H, carbamate α-CH_2), 4.53 (m, 1H, norbornyl-C(2)*H*). ^{13}C NMR ($CDCl_3$) δ 13.7 (carbamate ω-*C*H_3), 19.9 (carbamate β-*C*H_2), 24.2 (norbornyl *C*-6), 28.1 (norbornyl *C*-5), 32.1 (carbamate γ-*C*H_2), 35.2 (norbornyl *C*-7), 35.3 (norbornyl *C*-4), 39.6 (norbornyl *C*-3), 40.6 (norbornyl *C*-1), 41.6 (carbamate α-*C*H_2), 77.7 (norbornyl *C*-2), 156.4 (carbamate *C*=O). Mass spectra, exact mass: 211.157; elemental analysis: calculated for $C_{12}H_{21}NO_2$: C, 68.21; H, 10.02; N, 6.63, found C, 68.15; H, 10.32; N, 6.56. mp 178–180 °C) (decomp.).

(*R*)-(+)-*endo*- and (*S*)-(−)-*endo*-2-norbornyl-*N*–*n*-butycarbamates. ^{1}H NMR ($CDCl_3$) δ 0.92 (t, J = 7 Hz, 3H, carbamate ω-CH_3), 1.20–1.80 (m, 11H, carbamate β- and γ-CH_2 and 4,5,6,7-norbornyl *H*s), 1.96 (m, 1H, norbornyl C(1)*H*),

2.10–2.50 (m, 2H, norbornyl C(3)H_2), 3.19 (t, J = 7 Hz, 2H, carbamate α-CH_2), 4.60 (br. s, 1H, carbamate NH), 4.89 (m, 1H, norbornyl-C(2)*H*). ^{13}C NMR ($CDCl_3$) δ 13.7 (carbamate ω-*C*H_3), 19.8 (carbamate β-*C*H_2), 20.9 (norbornyl *C*-6), 29.4 (norbornyl *C*-5), 32.1 (carbamate γ-*C*H_2), 36.4 (norbornyl *C*-7), 36.9 (norbornyl *C*-4), 37.2 (norbornyl *C*-3), 40.4 (carbamate α-*C*H_2), 40.7 (norbornyl *C*-1), 75.7 (norbornyl *C*-2), 156.8 (carbamate *C*=O). Mass spectra, exact mass: 211.157; elemental analysis: calculated for $C_{12}H_{21}NO_2$: C, 68.21; H, 10.02; N, 6.63, found C, 68.17; H, 10.30; N, 6.58. mp 178–180 °C (decomp.).

2.3 Instrumental Methods

All steady state kinetic data were obtained from an UV–visible spectrophotometer (Agilent 8453) with a cell holder circulated with a water bath. ^{1}H, ^{13}C, and ^{19}F NMR spectra were recorded in $CDCl_3$ at 400, 100, and 377 MHz, respectively, with an internal reference tetramethylsilane (TMS) at 25 °C on a Varian Gemini 400 spectrometer. Mass spectra were recorded at 71 eV in a mass spectrometer (Joel JMS-SX/SX 102A). Elemental analyses were preformed on a Heraeus instrument. Optical rotation was recorded on a polarimeter (Perkin-Elmer 241).

2.4 Data Reduction

Origin (version 6.0) was used for linear and nonlinear least-squares curve fittings.

2.5 CEase Inhibition

CEase inhibition reactions were determined as described by Hosie et al. [9–11]. CEase-catalyzed hydrolysis of PNPB in the presence of a carbamate inhibitor was followed continuously at 410 nm on the UV–visible spectrometer. The temperature was maintained at 25.0 °C by a refrigerated circulating water bath. All reactions were preformed in sodium phosphate buffer (1 mL, 0.1 M, pH 7.0) containing NaCl (0.1 M), CH_3CN (2% by volume), detergent triton-X 100 (TX) (0.5% by weight), substrate PNPB (0.1 mM), and varying concentration of the inhibitors. Requisite volumes of stock solution of substrate PNPB and the inhibitor in acetonitrile were injected into reaction buffer via a pipet. CEase was dissolved in sodium phosphate buffer (0.1 M, pH 7.0). There was no pre-incubation of inhibitor and enzyme. The reaction was followed until 85% of substrate consumption was completed. Carbamate inhibitors (*R*)-(+)-*exo*-, (*S*)-(−)-*exo*-, racemic-(±)-*exo*-, (*R*)-(+)-*endo*-, (*S*)-(−)-*endo*- and racemic-(±)-*endo*-2- norbornyl-*N*–*n*-butylcarbamates were characterized as the pseudo or alternate substrate inhibitors of CEase (Scheme 1) [9–11, 17, 18]. The carbamylation stage was rapid compared to subsequent decarbamylation ($k_2 \gg k_3$), thus the two steps are easily resolved kinetically. The apparent inhibition constant ($1 + [S]/K_m$) K_i and carbamylation constant (k_2) were obtained from the nonlinear least-squares curve fitting of the k_{app} vs. [I] plot against Eq. (1) (Fig. 2). The inhibition constant K_i was then calculated form the apparent inhibition constant when both [S] and K_m values for the CEase-catalyzed hydrolysis of PNPB were known (Table 2). The K_m value for the CEase catalyzed hydrolysis of PNPB was 100 ± 20 μM obtained from Michaelis–Menten equation. The bimolecular rate constant, $k_i = k_2/K_i$, was related to overall inhibitory potency.

$$k_{app} = k_2[I]/(K_i(1 + [S]/K_m) + [I]) \quad (1)$$

In the presence of a carbamate inhibitor, time courses for hydrolysis of PNPB are biphasic, and k_{app} values can be calculated as Eq. (2) [9–11].

$$A = A_0 + (v_o - v_{ss})\left(1 - \exp\left(-k_{app}t\right)\right)/k_{app} + v_{ss}t \quad (2)$$

In Eq. (2), A_0, k_{app}, v_o, and v_{ss} are the absorbance at $t = 0$, the observed first-order inhibition rate constant, the initial velocity, and the steady-state velocity, respectively. Once k_{app} values have been determined as various inhibitor concentrations, the resulting data are fit to Eq. (1) to obtain K_i and k_2 values. The carbamylation stage is rapid compared to subsequent decarbamylation ($k_2 >> k_3$), thus the two stages are easily resolved kinetically.

Duplicate sets of data were collected for each inhibitor concentration.

2.6 Molecular Modeling

Molecular structures of (*R*)-(+)- and (*S*)-(−)-*exo*-2-norbornyl- *N*–*n*-butylcarbamates and (*R*)-(+)- and (*S*)-(−)-*endo*-2-norbornyl-*N*–*n*-butylcarbamates shown in Fig. 3 were depicted from the molecular structures after MM-2 energy minimization (minimum root mean square gradient was set to be 0.01) by CS Chem 3D (version 6.0).

3 Results and Discussion

3.1 Synthesis of (R)-(+)–exo-, (S)-(−)-exo-, (R)-(+)-endo-, and (S)-(−)-endo-2-norbornyl-*N*–*n*-butylcarbamates

(*R*)-(+)-*exo*-, (*S*)-(−)-*exo*-, (*R*)-(+)-*endo*-, and (*S*)-(−)-*endo*-2-Norborneols have been resolved by porcine pancreatic lipase in organic solvent (Schemes II & III) [6, 7]. The high amount of porcine pancreatic lipase used in these resolutions is due to the fact that porcine pancreatic lipase

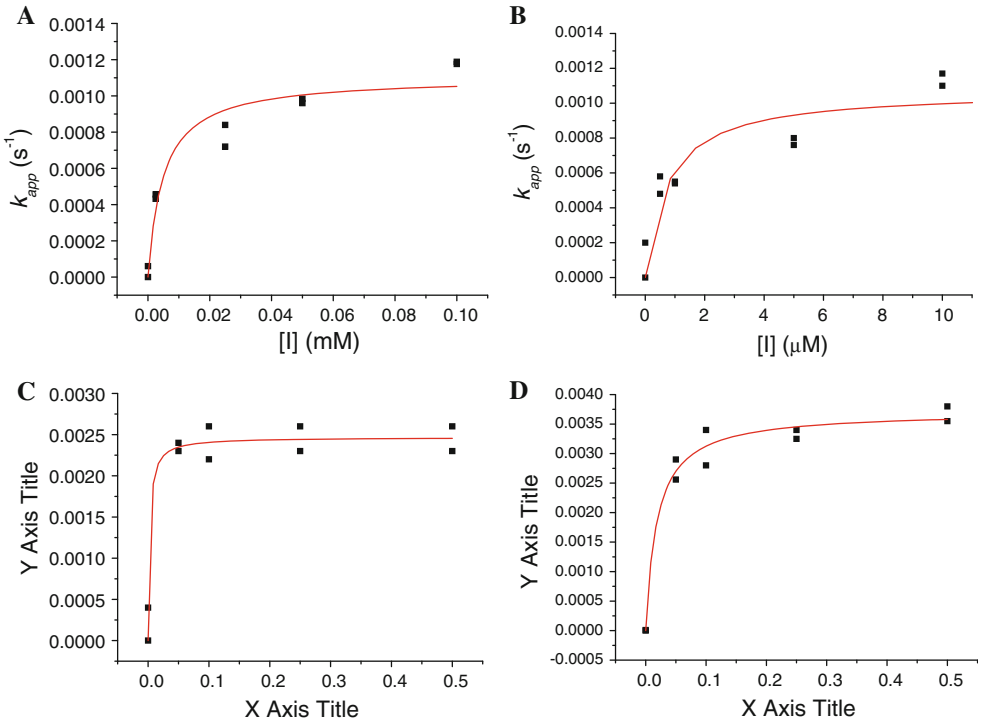

Fig. 2 Nonlinear least-squares curve fittings of k_{app} vs. inhibitor concentration ([I]) plot against Eq. (1) for the pseudo-substrate inhibition [9–11] of CEase by **a** (*S*)-(−)-*exo*-2-norbornyl-*N*–*n*-butylcarbamate, **b** (*R*)-(+)-*exo*-2-norbornyl-*N*–*n*-butylcarbamate, **c** (*S*)-(−)-*endo*-2-norbornyl-*N*–*n*-butylcarbamate, and **d**. (*R*)-(+)-*endo*-2-norbornyl-*N*–*n*-butylcarbamates. The parameters of the fit were **a** $k_2 = 0.0011 \pm 0.0001\ s^{-1}$, $K_i = 2.5 \pm 0.5\ \mu M$, and $R = 0.96995$; **b** $k_2 = 0.0011 \pm 0.0001\ s^{-1}$, $K_i = 0.4 \pm 0.1\ \mu M$, and $R = 0.96862$; **c** $k_2 = 0.0025 \pm 0.0001\ s^{-1}$, $K_i = 1.3 \pm 0.5\ \mu M$, and $R = 0.97909$; and **d** $k_2 = 0.0037 \pm 0.0001\ s^{-1}$, $K_i = 9 \pm 2\ \mu M$, and $R = 0.99099$. CEase-catalyzed hydrolysis of PNPB in the presence of carbamate was followed continuously at 410 nm on the UV–visible spectrometer at 25.0 °C. All reactions were preformed in sodium phosphate buffer (1 mL, 0.1 M, pH 7.0) containing NaCl (0.1 M), CH_3CN (2% by volume), detergent triton-X 100 (TX) (0.5% by weight), substrate PNPB (0.1 mM), and varying concentration of the inhibitors

Table 2 The k_2, K_i and k_i values of the CEase inhibitions by 2-norbornyl carbamates

Inhibitors	K_i (μM)	k_2 (10^{-3} s^{-1})	k_i (10^3 M^{-1} s^{-1})	Enantioselecitivity
(R)-(+)-*exo*-	0.4 ± 0.1	1.1 ± 0.1	3 ± 1	6.8
(S)-(−)-*exo*-	2.5 ± 0.5	1.1 ± 0.1	0.44 ± 0.08	1.0
rac-(±)-*exo*-	1.7 ± 0.1	1.2 ± 0.1	0.70 ± 0.07	1.6
(R)-(+)-*endo*-	9 ± 2	3.7 ± 0.1	0.41 ± 0.09	1.0
(S)-(−)-*endo*-	1.3 ± 0.5	2.5 ± 0.1	1.9 ± 0.7	4.6
rac-(±)-*exo*-	5 ± 1	3.2 ± 0.2	0.6 ± 0.1	1.5

K_i $(1 + [S]/K_m)$ values were obtained from the nonlinear least-squares curve fittings of k_{app} vs. [I] plot against Eq. (1) (Fig. 2) where [PNPB] = 100 μM and the K_m value for the CEase catalyzed hydrolysis of PNPB was 100 ± 20 μM which was calculated from Michaelis–Menten equation in the absence of any pseudo or alternate substrate inhibitor. The k_i values were calculated from k_2/K_i and uncertainty in k_i values = $\{(\text{uncertainty of } k_2)^2 + (\text{uncertainty of } K_i)^2\}^{1/2}$

catalytic rate in organic solvent is very slow. But isolation of product from the reaction mixture is easy for the enzyme reaction in organic solvent. The absolute configurations of (*S*)-(−)-*exo*-, (*R*)-(+)-*exo*- (Scheme 4), (*S*)-(−)-*endo*-, and (*R*)-(+)-*endo*-2-norborneols are determined on the basis of their optical rotation values and the ^{19}F NMR spectra of their Mosher's ester derivatives (Table 1).

Stereoisomers of (*R*)-(+)-*exo*-, (*S*)-(−)-*exo*-, (*R*)-(+)-*endo*-, and (*S*)-(−)-*endo*-2-norbornyl-*N*–*n*-butylcarbamates are synthesized from optically pure (*R*)-(+)-*exo*-, (*S*)-(−)-*exo*-, (*R*)-(+)-*endo*-, and (*S*)-(−)-*endo*-2-norborneols.

3.1.1 2-Norbonyl-N–n-butylcarbamates Act as Pseudo Substrate Inhibitors of Cholesterol Esterase

The mechanism for CEase-catalyzed hydrolysis of substrate involves formation of the noncovalent enzyme-substrate Michaelis complex, followed by nucleophilic attack

of the active site serine on the substrate, which leads to the acyl enzyme intermediate; hydrolysis of the acylenzyme completes the catalytic cycle (Scheme 1). In the presence of substrate, carbamates serve as the pseudo or alternate substrates inhibitors of CEase [9–11, 17, 18]. Accordingly, the carbamate inhibitors (Fig. 1) are characterized and the inhibition data are summarized in Table 2.

The first step for this pseudo substrate inhibition is reversible formation of the noncovalent enzyme-inhibitor complex, with inhibition constant K_i. Subsequent attack of serine residue of the enzyme on the carbamate carbonyl carbon of the inhibitor forms the carbamylenzyme, with rate constant k_2. The carbamate group of the inhibitor must bind to the acyl group binding site of the active site [4, 23], which is located deeply inside the enzyme. The third step is decarbamylation, governed by k_3.

3.2 Enantioselectivity for the CEase inhibitions by (R)-(+)- and (S)-(−)-exo-2-norbornyl-*N*–*n*-butylcarbamates (Table 2, Fig. 3a)

For the CEase inhibitions by *(R)*-(+)- and *(S)*-(−)-*exo*-2-norbornyl- *N*–*n*-butylcarbamates, *R*-enantiomer is 6.8 times more potent than *S*-enantiomer (Table 2). Therefore, CEase shows high enantioselectivity for *(R)*-(+)-*exo*-2-norbornyl- *N*–*n*-butylcarbamates over *(S)*-(−)-*exo*-2-norbornyl-*N*–*n*-butylcarbamate. Modeling both *(R)*-(+)-*exo*- and *(S)*-(−)-*exo*-2-norbornyl-*N*–*n*-butylcarbamates into the active site of CEase [4, 23] indicates that the norbornyl ring of *(R)*-(+)-*exo*-2-norbornyl-*N*–*n*-butylcarbamate is fitting well into the cholesteryl binding site of the enzyme (Fig. 3a). On the other hand, the norbornyl ring of *(S)*-(−)-*exo*-2-norbornyl-*N*–*n*-butylcarbamate is repulsive to Ser 194 and His 435 of the catalytic triad. This repulsion may create an unfavorable interaction between *(S)*-(−)-*exo*-2-norbornyl-*N*–*n*-butylcarbamate and the enzyme and make this inhibitor a less potent one.

When two most potent inhibitors *(R)*-(+)-*exo*-2-norbornyl-*N*–*n*-butylcarbamate and *(S)*-(−)-*endo*-2-norbornyl-*N*–*n*-butylcarbamate are compared, the norbornyl ring of *R-exo* isomer (Fig. 3b) is much closer to cholesteryl moiety of cholesterol ester than that of *S-endo* isomer (Fig. 3a). Therefore, the highly favorable interaction between the norbornyl ring of the inhibitor and the cholesteryl group binding site of the enzyme makes *(R)*-(+)-*exo*-2-norbornyl-*N*–*n*-butylcarbamate become the most potent inhibitors among four stereoisomers of 2-norbornyl-*N*–*n*-butylcarbamates (Table 2).

3.3 Enantioselectivity for the CEase inhibitions by (R)-(+)- and (S)-(−)-endo-2-norbornyl-*N*–*n*-butylcarbamates (Table 2, Fig. 3b)

For the PSL inhibitions by *(R)*-(+)- and *(S)*-(−)-*endo*-2-norbornyl-*N*–*n*-butylcarbamates, the *S*-enantiomer is 4.6 times more potent than the *R*-enantiomer (Table 2). Therefore, CEase shows high stereoselectivity for *(S)*-(−)-*endo*-2- norbornyl-*N*–*n*-butylcarbamates over *(R)*-(+)-*endo*-2-norbornyl-*N*–*n*-butylcarbamate from a similar reason (Fig. 3b).

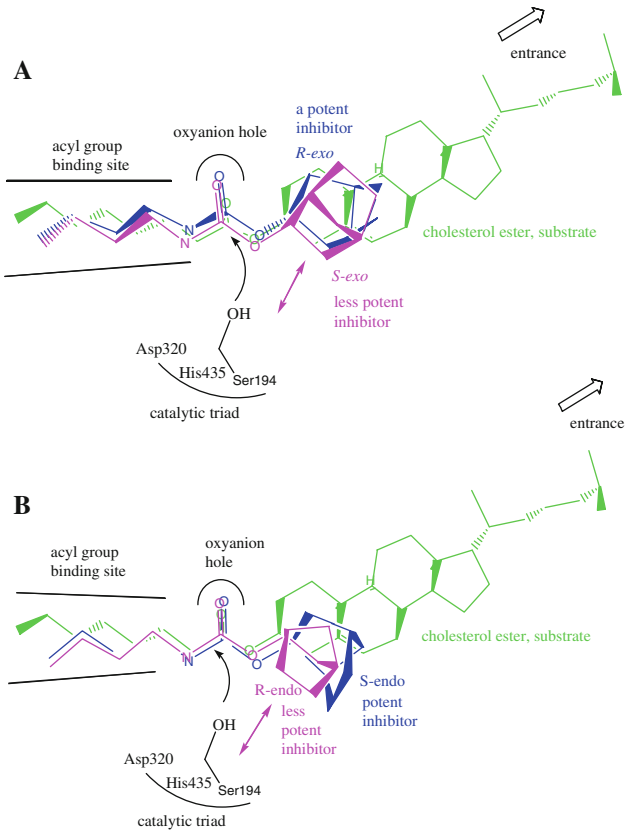

Fig. 3 Superimposition of (A) *(R)*-(+)- and *(S)*-(−)-*endo*-2-norbornyl-*N*–*n*-butylcarbamates, (B) *(R)*-(+)- and *(S)*-(−)-*exo*-2-norbornyl-*N*–*n*-butylcarbamates, and cholesterol ester at their carbamyl moieties or acyl group into the acyl group binding site of CEase [4, 23]. *R-exo* isomer is a more potent inhibitor than *S-exo* isomer due to an unfavorable, repulsive interaction between the norbornyl ring of *S-exo* isomer and the catalytic triad Ser 194. *S-endo* isomer is a more potent inhibitor than *R-endo* isomer due to an unfavorable, repulsive interaction between the norbornyl ring of *R-endo* isomer and the catalytic triad Ser 194

4 Conclusion

The stereoselectivity of CEase with respect to norbornyl-derived carbamates can be demonstrated for the first time. Among the four stereoisomers of the 2-norbornyl-*N*–*n*-butylcarbamates, *(R)*-(+)-*exo*-stereoisomer is the best inhibitor. It can therefore be concluded that unfavorable repulsions diminish the affinity when the *exo*-substituted inhibitor is *(S)*-configurated at the norbornyl moiety. For the *endo*-derivatives, an opposite conclusion can be drawn.

Acknowledgments We thank the National Science Council of Taiwan for financial support.

References

1. Auer J, Eber B (1999) J Clin Basic Cardiol 2:203–208
2. Berson JA, Walla JS, Remanick A, Suzuki S, Reynods-Warnhoff P, Willner D (1961) J Am Chem Soc 83:3986–3997
3. Brodt-Eppley J, White P, Jenkins S, Hui D (1995) Biochim Biophys Acta 1272:69–72
4. Chen JC-H, Miercke LJW, Krucinski J, Starr JR, Saenz G, Wang X, Spilburg CA, Lange LG, Ellsworth JL, Stroud RM (1998) Biochemistry 37:5107–5117
5. Chiou S-Y, Huang C-F, Yeh S-J, Chen I-R, Lin G (2010) J Enzym Inhib Med Chem 25:13–20
6. Chiou S-Y, Huang C-F, Yeh S-J, Chen I-R, Lin G (2010) Chirality 22:267–274
7. Chiou S-Y, Lai G-W, Lin L-Y, Lin G (2006) Ind J Biochem Biophys 43:52–55
8. Dale JA, Mosher HS (1973) J Am Chem Soc 95:512–519
9. Feaster SR, Quinn DM (1997) Meth Enzymol 286:231–252
10. Feaster SR, Lee K, Baker N, Hui DY, Quinn DM (1996) Biochemistry 35:16723–16734
11. Hosie L, Sutton LD, Quinn DM (1987) J Biol Chem 262:260–264
12. Hui DY (1996) Biochim Biophys Acta 1302:1–14
13. Irwin AJ, Jones JB (1976) J Am Chem Soc 98:8476–8482
14. Lopez-Candales A, Bosner MS, Spilburg CA, Lange LG (1993) Biochemistry 32:12085–12089
15. Maron DJ, Fazio S, Linton MF (2000) Circulation 101:207–213
16. Nakazaki M, Chikamatsu H, Naemura K, Asao M (1980) J Org Chem 45:4432–4440
17. Pietsch M, Gütschow M (2002) J Biol Chem 277:24006–24013
18. Pietsch M, Gütschow M (2005) J Med Chem 48:8270–8288
19. Pioruńska-Stolzmann M, Piroruńska-Mikołajczak A (2002) Pharm Res 43:359–362
20. Takahashi T, Fukuishima A, Tanaka Y, Takeuchi Y, Kabuto K, Kabuto C (2000) Chem Commun 788–789
21. Takahashi T, Kameda H, Kamei T, Ishizaki M (2006) J Fluorine Chem 127:760–768
22. Wang C-S, Hartsuck JA (1993) Biochim Biophys Acta 1166:1–19
23. Wang X, Wang C-S, Tang J, Dyda F, Zhang XC (1997) Structure 5:1209–1218
24. Winstein S, Trifan D (1951) J Am Chem Soc 74:1154–1160
25. Yoshizako F, Nishimura A, Chubachi M, Kirihata M (1996) J Ferm Bioeng 82:601–603